Annu. Rev. Nucl. Part. Sci. 1990. 40: 181–212

NEUTRINOS FROM SUPERNOVA EXPLOSIONS

A. Burrows

Departments of Physics and Astronomy, University of Arizona, Tucson, Arizona 85721

KEY WORDS: neutron stars, supernovae, stellar collapse.

CONTENTS

1. INTRODUCTION

Massive stars [$\gtrsim 8$ solar masses ($M_\odot$)] do not die quietly, but with dramatic and violent explosions that touch much of astronomy. With such "supernovae," neutron stars are born (1–3), the interstellar medium is enriched in the heavy elements of life and planets (4), energetic cosmic rays are created, and the cycle of stellar birth and death is renewed. Such a massive star lives for fewer than 3×10^7 years, becomes unstable within seconds, disassembles in hours or days, shines brightly in the optical for months to a year, and ends mixed in an expanding shell of ambient interstellar gas

0163–8998/90/1201–0181$02.00

that radiates x rays and radio waves for ten thousand years. In the Milky Way, this fabulous sequence of events is initiated approximately every fifty years (5–9), which with a galactic age of $\sim 10^{10}$ years implies that it has occurred as many as 10^8 times since our galaxy's creation.

Each one of these stellar deaths, neutron star births, and supernova explosions involves a series of extreme processes and events in the central $\sim 1.4 M_\odot$ of the doomed star whose matter-of-fact description can at times seem to border on hyperbole. However, as large as are the temperatures, densities, velocities, and accelerations achieved in the collapse and subsequent dynamics of that stellar core, it is the neutrino signature of these internal convulsions that jars the senses. Though the total optical radiations of a supernova amount to a respectable $\sim 10^{49}$ ergs and the kinetic energy of the expanding debris reaches $\sim 10^{51}$ ergs, the neutrino burst that lasts only seconds carries away more than 10^{53} ergs. This is equivalent to 0.1–0.2 solar masses, $\sim$50,000 Earth masses, or $\sim 5 \times 10^{30}$ megatonnes of TNT. For those few seconds, the neutrino luminosity of a single supernova can rival the total optical emissions of the entire observable universe. Averaging these bursts over the millenia, the galaxy's neutrino luminosity is comparable to its optical luminosity. During our galaxy's life, $\sim 10^7 M_\odot c^2$ of neutrinos have issued from neutron star births. This is equivalent to the mass of 10 giant globular clusters of $\sim 10^6$ stars each. Since the speed of light (neutrinos) is finite, there are 10–100 solar masses of burst neutrinos in very thin expanding shells within our galaxy at any one time.

In this review, we focus on the physics of these supernova neutrinos. Other reviews of this subject can also be found (10–13). Since such neutrinos are thought to originate only from the cores of massive stars as they die, we ignore those supernova explosions that are primarily thermonuclear in nature (e.g. Type Ia). Henceforth, when we refer to supernovae, we implicitly mean core collapse supernovae (14) (e.g. Type II or perhaps Type Ib). This subject was electrified three years ago by the detection of the neutrino burst from the Type II supernova, SN1987A, in the Large Magellanic Cloud (LMC), approximately 50 kiloparsecs away (15–23). These first-of-their-kind neutrino observations not only ushered in extragalactic neutrino astronomy, but capped almost thirty years of steady theoretical progress that had until that time been conducted in sterile isolation. The good correspondence between the modern theory, built on decades of research, and these new neutrino observations should not lull us into smug satisfaction. With only a handful of neutrino events from SN1987A, the most interesting predictions of supernova theory were not tested. Thus, in this review we place special emphasis on the untested features of neutrino bursts that will speak eloquently when such a burst is

next detected on Earth. Neutrinos are produced in abundance at the temperatures and densities achieved during stellar collapse, and their weak coupling to matter ensures a rich yield at infinity, despite a thick stellar mantle that is profoundly opaque to photons. Therefore, in principle, it is the distinctive luminosity evolution, spectra, and flavor mix of the penetrating neutrinos that will allow us finally to diagnose stellar collapse in detail.

2. EARLY HISTORY

The several ingredients of supernova theory include nuclear physics, statistical mechanics, weak interaction physics, general relativity, hydrodynamics, and transport theory. Hence, it should come as no surprise that progress in our understanding of the supernova phenomenon has paralleled the progress of physics during the last fifty years.

Landau in 1932 (1) was one of the first to suggest that a star could be supported against gravity by the degeneracy pressure of neutrons, just as white dwarfs are supported by the degeneracy pressure of electrons (24). In 1934, the large gravitational binding energy of such a wildly compact star inspired Baade & Zwicky (2) to connect supernova explosions with neutron stars. During roughly the same time, Chandrasekhar (24) was concluding that special relativity and quantum mechanics together implied that white dwarfs possess a maximum mass ($\sim 1.4 M_{\odot}$), above which they will experience gravitational collapse. As important as these developments were, the field came into its own only after World War II, with the explosion of nuclear knowledge and the advent of computers and large-scale numerical simulation. In 1957, the landmark paper of Burbidge, Burbidge, Fowler & Hoyle (4) introduced the onionskin structure of massive stars and a comprehensive theory for the origin of the elements by progressive stages of thermonuclear burning. They also made the connection between core thermonuclear exhaustion, core collapse, and supernova explosions—a connection that survives, in broad outline, today. The mechanism of explosion was thought to be the collapse-induced thermonuclear detonation of oxygen (25–27), produced during the quiescent stellar burning stages. However, Chiu (28, 29) showed that neutrinos would be copiously produced during the hot, late stages of stellar evolution and stellar collapse, and this led Colgate & White (30) and Arnett (31, 32) to perform the first hydrodynamic simulations of core collapse and explosion that contained the essential elements of any credible modern attack: a good progenitor model, neutrino transport, a nuclear equation-of-state (EOS), and numerical acumen. The essential connection between stellar death and core collapse, neutron star formation, and supernova explosions

was permanently forged in these seminal works. Along with the work of Colgate & Johnson (33), these papers started the debate between the purely hydrodynamic and the neutrino energy transfer models of supernovae that still rages in this the last decade of the twentieth century.

The debate now rages at a more sophisticated level, however, since significant advances have been made in the EOS of nuclear matter (34–41), in neutrino physics (28, 29, 42–49), and in our knowledge of the mass, structure, and evolutionary history of the progenitor stars (50–54).

3. DESCRIPTION OF STELLAR COLLAPSE

In order fully to understand the supernova neutrino light curve, the features and quantities of collapse and explosion must be laid out. Here, we sketch stellar evolution and core dynamics and establish a context for the subsequent discussion.

Stellar evolution is a constant battle between pressure and gravity. The ignition of a thermonuclear fuel temporarily halts the gravitational collapse of a star that would otherwise be driven by energy loss to contract. As each fuel is exhausted, the stellar core does indeed slowly contract and, by compression, increase its temperature. For all but the lightest stars, this compression ignites the ashes of the previous fuel cycle. In this way, the cores of stars evolve through successive stages of temperature and density increases and higher atomic weights. A structure of nested shells of progressively lighter elements from the center outward is established: the so-called onionskin structure (4, 14). The cores of stars between $1M_{\odot}$ and $\sim 8M_{\odot}$ evolve from hydrogen to helium, and then from helium to carbon and oxygen. At this stage, an envelope instability bares the ~ 0.5–$1.0M_{\odot}$ white dwarf core and truncates the burning sequence (55). The star ends its life as a "planetary" nebula with a white dwarf remnant, supported against collapse by the zero-point pressure of electrons and, barring later accretion from a companion, with no thermonuclear future. However, the rarer, more massive stars ($\gtrsim 8M_{\odot}$) continue burning to heavier elements and accumulating degenerate cores that approach the critical Chandrasekhar limit. The lighter ($<10M_{\odot}$?) massive stars grow oxygen-neon-magnesium cores, and the heavier ($>10M_{\odot}$?) ones grow iron cores, but the cores of all massive stars reach the Chandrasekhar limit before any envelope instability arises (14). Note that iron is at the peak of the nuclear binding energy curve and that when silicon burning to iron is completed, no more thermonuclear fuel is available in the core.

The convergence of the stellar cores to a narrow range of similar masses around the classical Chandrasekhar mass, despite the wide range ($8M_{\odot} \lesssim M \lesssim 60M_{\odot}$) of progenitor total masses, is a consequence of neu-

trino cooling by pair, plasmon, and photoneutrino processes (45, 46, 56, 57). At the high central temperatures and densities achieved during and after carbon ignition, these core neutrinos dominate surface photons as energy sinks, but their average energy (<1 MeV) and luminosity ($<10^{49}$ ergs s^{-1}) are still too low to be detected by reasonable technology. They ensure that the entropy of the core is low ($s \approx 1$ per baryon per Boltzmann's constant) and hence that it is in a thermodynamically well-ordered and near-degenerate state. This forces the electron zero-point pressure to dominate the total pressure and the core to behave as a white dwarf. Since white dwarfs cannot exceed the Chandrasekhar mass, a natural mass scale is introduced into the stellar evolution, supernova, and neutron star birth problems. When the core reaches a Chandrasekhar mass, stellar collapse begins.

The unstable core is near $\sim 1.4 M_\odot$, has a radius of a few thousand kilometers, and is embedded in a star with a radius of between 10^7 and 10^9 kilometers. Therefore, it is geometrically unprepossessing. However, its initial central temperature (T_c) and density (ρ_c) are near 5×10^9 K (~ 0.5 MeV) and 10^{10} g cm^{-3}, respectively, and the electrons are relativistic, with an initial central chemical potential energy (μ_e) near 10 MeV (50, 52–54). When the core starts to implode, a rarefaction wave is sent into the stellar envelope, but at a speed that is significantly smaller than the speed of collapse. Therefore, during collapse and explosion, the envelope can be considered static. It is the core that collapses, not the entire star.

Because of either the endothermic photodissociation of iron (4) or electron capture on core nuclei (either iron or Ne-Mg) (28, 29), the effective adiabatic index (γ) goes below the critical 4/3 of an ideal, relativistic electron gas. The core loses pressure support and implodes homologously (58) [velocity (v) $\propto$ radius (r)]. As the collapse proceeds, the flow breaks up into a subsonic inner core ($M \approx 0.5$–$0.7 M_\odot$) and a supersonic outer core ($M \approx 0.9$–$0.7 M_\odot$), separated by a sonic point (59). The maximum collapse velocities are achieved at an intermediate core radius, near the moving sonic point, and not at the center or the periphery. When the subsonic inner core reaches nuclear densities ($\rho_N \approx 2.7 \times 10^{14}$ g cm^{-3}), a nuclear phase transition between bound nuclei and free nucleons occurs (36, 38, 39, 60, 61). This transition is crucial to core dynamics. Before it, the soft ($\gamma \leq 4/3$) relativistic electrons (and electron neutrinos) dominate the pressure and cannot halt collapse. After it, the repulsive, nonrelativistic, nucleons dominate the pressure and the inner core stiffens dramatically. It rebounds as a unit into the unsuspecting supersonic outer core and a shock wave is generated at the interface between them (62–67). Starting at a radius of ~ 20 kilometers, a matter density of 10^{13-14} g cm^{-3}, an interior mass of ~ 0.5–$0.7 M_\odot$ (68–70), and a speed near 10^{10} cm s^{-1} ($\sim c/3$), the

shock entropizes and dissociates (70–72) the outer mantle as it works its way out in mass and radius, possibly itself to become the supernova explosion. The generation of entropy indicates the irreversibility of the dynamics. Not all the core can rebound to infinity.

The expanding inner core energizes the shock wave by doing "PdV" work on the outer zones of the core and achieves hydrostatic equilibrium within milliseconds of bounce (65). A "protoneutron star" with a low entropy ($s \approx 1$) core and a high entropy ($s \approx 8$–10) mantle is formed (3, 63, 71–74). At this stage, it continues to be fattened by the further accretion of outer core matter (75, 76) and is bounded by the shock wave that is at a radius of 200 km within 10 ms. Either the shock continues undeterred into the outer stellar envelope or it stalls, only to be revived within hundreds of milliseconds to seconds by neutrinos from the core. These are the so-called prompt (33, 38, 67, 77) and delayed (74, 75, 78–80) mechanisms respectively of core collapse supernovae. Whichever obtains, the proto-neutron star is a central focus of supernova theory. A schematic synopsis of the evolution described above is given in Figure 1.

Core collapse to nuclear densities takes less than one second, but most of the dynamical action occurs in the last phases before bounce. To go from $\rho_c = 10^{10}$ to 10^{11} g cm^{-3} takes $\sim$100 ms, from 10^{11} to 10^{12} g cm^{-3} takes $\sim$25 ms, from 10^{12} to 10^{13} g cm^{-3} takes $\sim$5 ms, and from 10^{13} to 10^{14} g cm^{-3} takes only $\sim$1 ms (13, 81, 82). Such accelerating compression is accompanied by a change in the central temperature from $\sim$0.5 MeV at instability to 10 MeV at bounce ($T_c \approx \rho_c^{0.2-0.25}$) (64, 67, 83, 84). During bounce and shock formation, accelerations of 10^{14} cm s^{-2} ($\sim 10^{11}$ g) and velocities of 8×10^9 cm s^{-1} ($\sim c/4$) are achieved (64). Because of the enormous compressions, μ_e reaches $\sim$300 MeV and the chemical potential of the electron neutrino (μ_{ν_e}) reaches $\sim$200 MeV. The high neutrino energies and matter densities result in an integrated Rosseland mean opacity to the electron neutrino from the center to infinity of 10^{4-5} ($\gg 1$) (3). Such high neutrino opacity is an exotic and distinguishing feature of protoneutron star physics.

4. NEUTRINO TRANSPORT

Neutrino transport involves the creation, absorption, scattering, and flow of neutrinos of all the six known neutrino species (ν_e, $\bar{\nu}_e$, ν_μ, $\bar{\nu}_\mu$, ν_τ, $\bar{\nu}_\tau$). The

Figure 1 A schematic (not to scale) depicting the evolution of the core of a massive star like the progenitor of SN1987A from core collapse to bounce and shock formation, to protoneutron star, to young, compact neutron star. Neutrino radiation is indicated with ν's and mass accretion with $\dot{M}$'s.

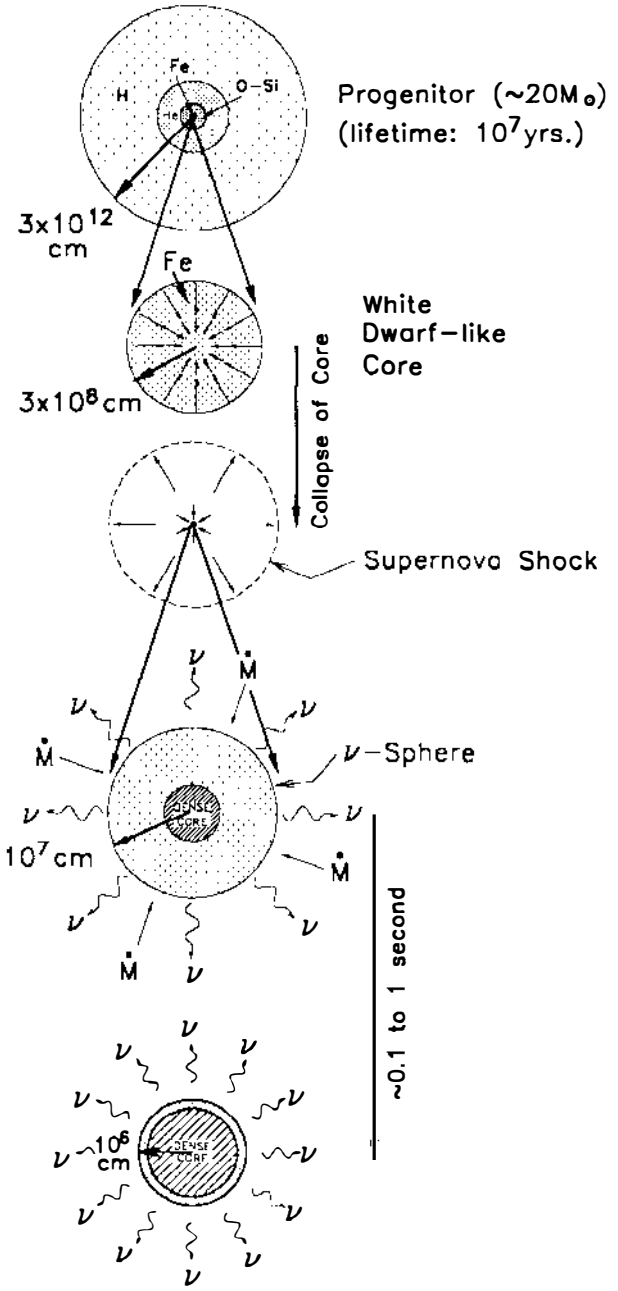

energy, momentum, and lepton number flows of these neutrinos play pivotal roles in the dynamics and thermodynamics of the core after the onset of collapse. In this section, we summarize some of the weak interaction and neutrino processes that are important in supernova physics and highlight the most pertinent facets of the neutrino-matter coupling. The neutrino emissions at infinity indirectly bear the stamp of these processes in the core.

4.1 *Sources*

The core is composed of alpha particles, heavy nuclei, nucleons, electrons, positrons, photons, and neutrinos in thermal and nuclear statistical equilibrium (61). The precise abundances of each species depend only upon the standard thermodynamic quantities [density (ρ), temperature (T), and composition] and can be calculated using the chemical potential equilibrium conditions (38, 85). The neutrino source terms depend sensitively on the thermodynamic conditions of the matter.

4.1.1 CAPTURE At the low entropies of the imploding core, nuclei are not dissociated before bounce, and shock formation and the free-proton mass fractions are kept low ($10^{-5} < Y_p < 10^{-2}$) (41). Nevertheless, there are sufficient protons that the superallowed electron-capture process, $e^-(p, n)\nu_e$, can compete with electron capture on the mix of ambient nuclei, initially with atomic weights near that of iron (or O-Ne-Mg), in producing capture ν_e's. The Fermi energies of the electrons ($\mu_e \geq 10$ MeV) certainly exceed the $\sim$1-MeV thresholds of these processes, but the dominant nuclei and transitions and their beta strengths have not yet been clearly identified, though they have been intensively studied (38, 86–90). Be that as it may, capture ν_e's with progressively increasing average energies and at progressively increasing rates ($\propto Y_p \mu_e^5$ for free protons) stream out to announce the first phase of supernova neutrino emission. Capture ν_e's dominate during infall and signal the initial neutronization of the core as it begins its transformation into a neutron star.

After the ν_e's become trapped (91–93) in the flow, however (see Section 4.3), the inverse reaction, $\nu_e(n, p)e^-$, becomes important and stabilizes net electron lepton (hereafter, "lepton") loss. A beta equilibrium is established in which ν_e and e^- capture are balanced and a new conserved composition variable, the lepton number per baryon ($Y_\ell = Y_e + Y_{\nu_e}$), is introduced. Because of the new thermodynamic constraint of beta equilibrium, Y_ℓ replaces Y_e as the appropriate composition variable of the matter. Thereafter, the matter is completely characterized by T, ρ, and Y_ℓ. Though the individual capture rates can be quite large after $\rho = 10^{12}$ g cm^{-3} is achieved, the introduction of beta equilibrium and the conserved com-

position variable Y_ℓ makes the actual magnitude of the capture rates irrelevant to the subsequent neutrino signal and the evolution. Before trapping, the actual rate is important in determining the rate of collapse, since capture is then undermining the electron pressure support of the core.

4.1.2 PAIR PRODUCTION During collapse, the temperatures and densities are still too small to produce a competing number of ν_μ's, $\bar{\nu}_\mu$'s, ν_τ's, $\bar{\nu}_\tau$'s (hereafter called ν_μ's), or $\bar{\nu}_e$'s by the neutral-current e^+e^- annihilation, plasmon decay, or photoneutron pair production processes (45, 46, 56, 57). In addition, $\bar{\nu}_e$ production by positron capture is suppressed by the large electron fraction ($Y_e \approx 0.4$–0.5) and consequently large and positive μ_e ($\gg m_e c^2$).

However, as the core reaches nuclear densities and temperatures near 10 MeV, the ν_μ production rates skyrocket. The time scale to fill the blackbody seas of ν_μ's becomes smaller than the dynamical and diffusion times. Here again, all that is important is that an equilibrium population of ν_μ's can be produced. The precise production rates do not matter because after a blackbody sea has been filled, the inverse processes of neutrino pair annihilation stabilize it. Note that the ν_μ's begin to be produced copiously only after the matter becomes opaque to them. Therefore, even during bounce, there is little ν_μ emission to infinity. It is only after the hot shock wave has reached low densities ($\lesssim 10^{12}$ g cm^{-3}) and the neutrino-transparent region that ν_μ's start to leak out and contribute to the neutrino signature. The production of ν_μ's to become an important component of the supernova neutrino saga is a direct consequence of the existence of neutral currents (46, 56, 57), since muon and tau production are greatly suppressed by their large rest masses (31, 77).

The $\bar{\nu}_e$'s are also produced in the hot, dense core and achieve thermal equilibrium. However, unlike the ν_μ's, which have zero chemical potential, the trapped ν_e's have a chemical potential that reaches $\sim$200 MeV at bounce. Therefore, the $\bar{\nu}_e$'s are severely Boltzmann-suppressed in the core. The $\nu_e/\bar{\nu}_e$ asymmetry is a direct consequence of the e^-/e^+ asymmetry, electron-lepton conservation, and trapping. Almost no $\bar{\nu}_e$'s exist deep in the core during the entire multisecond evolution from collapse to "cold" neutron star. It is only at the periphery of the protoneutron star, just interior to the boundary between opacity and transparency, that significant numbers of $\bar{\nu}_e$'s can exist. It is there that rapid ν_e loss drastically lowers $\eta_{\nu_e} = \mu_{\nu_e}/T$ and lifts the suppression of significant numbers of $\bar{\nu}_e$'s. Interestingly, the opacity of the object still creates a standard $\bar{\nu}_e$ emission surface that conceals core $\bar{\nu}_e$ suppression from view.

In sum, since the mean free paths of neutrinos in supernova cores become short very quickly, the importance of the neutrino source terms

lies not in the specific rates, but in the fact that they can operate on time scales short compared to diffusion and dynamical times and hence can guarantee blackbody seas. Diffusion, not production, determines the salient features of the supernova neutrino signal.

4.2 *Neutrino Opacity*

Stellar collapse is the only astrophysical context, after the big bang, in which neutrino opacity is an issue. Neutrinos are notoriously "weakly" interacting. However, at the high densities and neutrino energies achieved during and after collapse, the neutrino mean free paths become short and the star is no longer transparent. This has been known for decades, but since it was first recognized (30, 31) our understanding of both stellar collapse and the physics of the weak interaction has evolved significantly (13). An important milestone in supernova studies was the discovery of the weak neutral current (46–48, 94). It introduced new scattering and production processes for neutrinos and allowed ν_μ's to be generated in the core in abundance. Neutrino opacity directly regulates neutrino losses, the dynamics of stellar collapse, and the neutrino signals in terrestrial detectors.

The major sources of opacity that must be incorporated into collapse and protoneutron star simulations are

$$\nu_i + \mathrm{A} \rightarrow \nu_i + \mathrm{A} \qquad \text{1a.}$$

$$\nu_i + (\mathrm{n}, \mathrm{p}) \rightarrow \nu_i + (\mathrm{n}, \mathrm{p}) \qquad \text{1b.}$$

$$\nu_i + \mathrm{e}^- \rightarrow \nu_i + \mathrm{e}^- \qquad \text{1c.}$$

$$\nu_\mathrm{e} + \mathrm{n} \rightarrow \mathrm{e}^- + \mathrm{p}, \qquad \text{1d.}$$

where n and p represent unbound neutrons and protons, respectively, and ν_i denotes a neutrino of species i. Process 1a represents coherent scattering by a nucleus of atomic weight, A. Both processes 1a and 1b involve purely neutral-current elastic scattering whose cross sections are species-independent (47–49). Process 1c has charged- and neutral-current terms for ν_e's and $\bar{\nu}_\mathrm{e}$'s, and only neutral-current terms for ν_μ's (94). Process 1d is the inverse of electron capture and has only a charged-current component. The opacities of the four processes (in $\mathrm{cm}^2\ \mathrm{g}^{-1}$) are given roughly by

$$\kappa_\mathrm{a} \approx 3 \times 10^{-20} \left(\frac{\varepsilon_\nu}{\mathrm{MeV}}\right)^2 \left(\frac{A}{56}\right) \qquad \text{2a.}$$

$$\kappa_\mathrm{b} \approx 10^{-20} \left(\frac{\varepsilon_\nu}{\mathrm{MeV}}\right)^2 \qquad \text{2b.}$$

$$\kappa_c \approx 10^{-21}\left(\frac{\varepsilon_\nu}{\text{MeV}}\right) \qquad (\nu_e\text{-}e^- \text{ only}) \qquad 2c.$$

$$\kappa_d \approx 2 \times 10^{-20}\left(\frac{\varepsilon_\nu}{\text{MeV}}\right)^2, \qquad 2d.$$

respectively, where κ_c is the opacity for ν_e-e^- scattering alone (for ν_μ-e^-, it is $\sim 1/6$ of this), and ε_ν is the neutrino energy. It was assumed in Equation 2b that all baryons are in nucleons (high s) and in Equation 2a that all baryons are in nuclei (low s). For simplicity and demonstration purposes, all final-state Pauli blocking is ignored. In reality, the Pauli exclusion principle can decrease the cross sections of processes 1b (3, 95–98), 1c (99, 100), and 1d (3, 101) by different factors that depend upon ρ, T, and Y_e. The coherent scattering process 1a dominates the opacity of all species during infall when most of the baryons are locked in nuclei (38, 102, 103). Above the phase transition near nuclear densities and at high shock-induced entropies, the baryons are in free nucleons and processes 1b and 1d (for ν_e's) dominate. Because of the large energy transfer per collision and despite the small cross section, the inelastic electron-scattering process 1c is important in the energy equilibration and thermalization of all species (66, 83, 84).

The profoundly weak coupling of neutrinos to matter is made clear when Equation 2a at $\varepsilon_\nu = 1$ MeV and $A = 56$ is compared with the Thomson scattering opacity (γ-e^-), $\kappa_T \approx 0.2$ cm^2 g^{-1}. The nineteen orders of magnitude between them suggests that neutrinos rarely encounter obstacles. However, in supernovae, densities as high as 10^{15} g cm^{-3} are achieved. Since all the dominant neutrino opacities are monotonically increasing functions of ε_ν and compression and heating during collapse produce high ε_ν's ($0 < \varepsilon_\nu \lesssim 200$ MeV), the high ρ's and ε_ν's combine to render the core opaque to all neutrino species early during infall. Specifically, when $\rho_c = 10^{11}$ g cm^{-3}, ε_{ν_e} is near 10 MeV and we derive a mean free path, λ_a ($= 1/\kappa_a\rho$), of ~ 30 kilometers. This is smaller than the ~ 100-km radius of the core at this early phase of collapse (64, 104) and demonstrates that the ν_e's being produced in electron capture can no longer stream out unimpeded. They are becoming trapped in the flow. Similar arguments can be applied to the other species and we see that, long before nuclear densities are reached, neutrino diffusion, not free escape, governs and throttles the neutrino losses. In detailed protoneutron star calculations (3, 98), the mean free path of the ν_e shrinks to ~ 1 meter in the center! The observed long duration of the SN1987A signals is a direct consequence of this neutrino opacity.

4.3 *Trapping*

There is sufficient confusion about the term "trapping" that a few words of clarification are in order. Trapping does not refer to the opacity of the core to neutrinos. It has been a tenet of the theory since its inception that the neutrino mean free paths were smaller than the core and that some form of neutrino diffusion obtained (31, 77). However, early researchers thought that the imploding core neutronized through electron capture early during the collapse. Therefore, in their simulations, they assumed a priori that the matter was neutron-rich (proton- and electron-poor). In the modern theory, this is not the case. Mazurek (91, 105–107) and Sato (92) independently pointed out that during infall, at the same time central densities of $\sim 10^{11}$ g cm^{-3} are being reached and the rapidly increasing electron-capture rates are threatening to neutronize the core completely, the matter is becoming opaque to the capture electron neutrinos. Instead of being lost to infinity, these electron neutrinos are trapped in the imploding flow and the loss of leptons is thwarted. The reverse process of ν_e capture stabilizes electron loss and the lepton number per baryon is conserved at a value ($Y_\ell \approx 0.33$–0.4) (63, 66, 69, 75, 83, 84, 108) only slightly below its precollapse value ($Y_e \approx 0.4$–0.5; $Y_{\nu_e} = 0$) (14). The conserved lepton fraction (Y_ℓ) is the new composition variable. At a given T, ρ, and Y_ℓ, Y_e and Y_{ν_e} are set by the constraint of beta equilibrium. Trapping is the trapping of lepton flavor early during collapse. As an historical note, Mazurek derived trapping without neutral currents and employed the 1964 ν_e-e$^-$ scattering cross sections of Bahcall (43).

The consequences of trapping are manifold. Frustrating energy loss by neutrino radiation and achieving chemical equilibrium make the dynamics adiabatic early on. That much of the infall occurs at a constant, low entropy and constant composition is a great conceptual simplification. The low entropies and high electron numbers ensure that neutrons stay in nuclei during collapse. They are neither evaporated by high temperatures nor are they dripped by high neutron excesses. As a consequence, the "soft" relativistic electrons and ν_e's continue to dominate the pressure, and the core remains unstable all the way to nuclear densities (35–38, 61, 85, 109). Only then does the phase transition from nuclei to nucleons finally liberate abundant "stiff," nonrelativistic nucleons to dominate the pressure and halt collapse. Furthermore, because of trapping, the fermionic ν_e's become degenerate, with chemical potentials μ_{ν_e} that reach ~ 200 MeV near bounce. Their transport becomes oddly similar to that of the degenerate electrons in a normal terrestrial metal (73).

If trapping did not occur, the gravitational energy of collapse would be channeled into the thermal energy of the free nucleons, the bounce would

be reversed significantly below nuclear densities (31, 77), and the average ν_e energy at bounce would be significantly lower than in the modern model. As a result, the core at bounce would be much less opaque to neutrinos, and hence the characteristic neutrino diffusion times would be as much as one or two orders of magnitude shorter. Importantly, trapping converts what would be a neutrino burst of a few hundred milliseconds into a burst of many seconds, much like the neutrino burst observed from SN1987A.

4.4 *Neutrino Transport Techniques*

The neutrinos carry energy, momentum, and lepton flavor and the solution of their transfer equations is as important in the study of supernovae and neutron star birth as is the solution of the equations of hydrodynamics. The two are intimately coupled in a highly nonlinear fashion. The techniques for the solution of these coupled partial differential equations have evolved significantly over the past thirty years, but a detailed recounting of this history would be out of place in this review. A multitude of approaches, at various levels of approximation, have been used to solve the general problem. Rosseland mean-diffusion (31, 32, 110–118), angle-integrated multi-energy group (41, 75–77, 83, 84, 93, 102, 119, 120), full radiative transfer (121–126), and Monte Carlo (100, 127, 128) schemes have all been developed.

Today, a relatively clear picture has emerged concerning the spectra, luminosities, and types of neutrinos emitted from the variety of artificial cores provided by the stellar evolution community (14, 50, 52–54). The differences from one core model to the next are not as important as the similarities and the fact that there has been a general convergence of theory since the seminal work of the 1960s. This is not to say that there are no ambiguities or unsolved problems. There is as yet no strong consensus for the actual mechanism of the supernova explosion (39, 41, 67, 78–80, 129). However, such has been the recent progress of the theory that even this question seems to have been reduced to an argument over details.

5. THE NEUTRINO SIGNAL

Having developed the vocabulary and the context of the neutrino signature of core collapse supernovae, we can now describe it and its salient features. An extensive literature has developed over the years concerning the luminosities, spectra, mix of neutrino species, and neutrino discriminants of the various supernova mechanisms, some of it quite useful (e.g. 3, 73, 76, 98, 130–140). Since it was first realized that neutrinos would be a good probe of supernova cores (141, 142), these quantities have changed

drastically (13). SN1987A was not the theoretical supernova of the 1960s. However, we do not review that history here, nor do we describe all the modern results with the variety of progenitors stars that have been employed. Rather, we focus on a few baseline calculations illustrating the central features of the neutrino emissions, in the hope that what is truly generic will become clear to the reader. Some good, alternate but recommended, theoretical treatments can be found in (75, 76, 143, 144).

5.1 *Infall, Breakout, and Early Protoneutron Star Phases*

Figure 2, taken from Myra & Burrows (120), depicts the ν_e, $\bar{\nu}_e$, and ν_μ (all four species) luminosities during the most interesting dynamical phases of collapse, from about 10 ms before bounce to about 100 ms after bounce. The onset of collapse was at $t = 0$. For this calculation, the $1.17M_\odot$ iron core from the $13M_\odot$ progenitor star of Nomoto & Hashimoto (145) was employed. Electron capture to a core value of $Y_e = 0.41$ before collapse and the Coulomb correction to the electron pressure are responsible for such a small effective Chandrasekhar mass, which can vary from $\sim 1.2M_\odot$

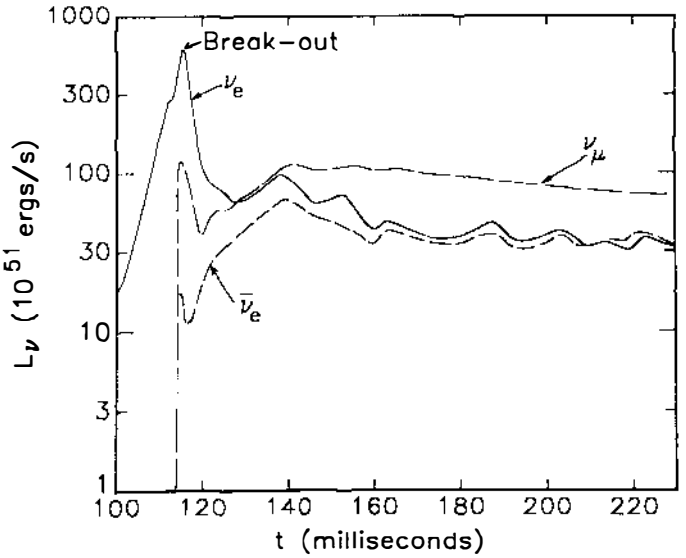

Figure 2 The neutrino luminosity (in 10^{51} ergs s^{-1}) versus time (in milliseconds) for $\bar{\nu}_e$, ν_e, and ν_μ neutrino types through the first ~ 100 ms after bounce [from Myra & Burrows (120)]. Time was set equal to zero at the onset of the collapse of the $1.17M_\odot$ model from Nomoto & Hashimoto (145). Notice the sharp spikes in the $\bar{\nu}_e$, ν_μ, and ν_e curves, the "slow" rise of the ν_μ and $\bar{\nu}_e$ curves after turn-on, and the oscillations. See text for a discussion of the salient features of this plot.

to $2.0 M_{\odot}$ as a result of the Y_e and entropy variations possible from model to model (14, 54).

As Figure 2 shows, ν_e emission predominates during infall, increasing at the last stages before bounce almost exponentially with a time constant of $\sim$4.6 ms. The average energy of infall ν_e's is $\sim$10 MeV and is set by the slowly varying electron chemical potential ($\mu_e \propto \rho^{1/3}$) at trapping density ($\rho \approx 10^{11-12}$ g cm^{-3}). The spectrum is a capture spectrum, not a thermal or quasi-thermal spectrum, and can in principle be quite complicated since it reflects an unknown combination of electron capture on free protons and exotic nuclei (88–90). Nevertheless, in this calculation $\sim 1.3 \times 10^{51}$ ergs in ν_e's are radiated before bounce. This is less than 1% of the binding energy of the final neutron star (~ 2–3×10^{53} ergs) that will eventually emerge as neutrinos of all species. Such a small percentage is predominantly a consequence of trapping, and the verification of this central prediction of the standard model should be a goal of future burst searches. Approximately 50 events in both the Sudbury Neutrino Observatory (SNO) heavy-water detector (146), and the ICARUS argon detector suggested for the Gran Sasso tunnel (147) are predicted during this phase from a core collapse supernova two kiloparsecs away (13). Light-water Čerenkov detectors such as Kamiokande II (148, 149) are only $\sim$1/8 as sensitive to these ν_e's.

Bounce occurs at $\sim$113 ms near the slight kink in the L_{ν_e} curve in Figure 2. Though formed in the neutrino-opaque region, the bounce shock quickly speeds out to lower densities and greater radii and only $\sim$1 ms after bounce breaks out through the electron neutrinosphere. A neutrinosphere is the boundary between neutrino-transparent and neutrino-opaque regions and is strictly analogous to the classic photosphere (the emission surface) of stars. As Figure 2 shows, shock breakout is accompanied by a prodigious burst of ν_e's whose luminosity reaches $\sim 6 \times 10^{53}$ ergs s^{-1}. The brief breakout burst of ν_e's is a distinctive signature of shock propagation that is supplied by the ν_e's from rapid electron capture on the newly shock-liberated protons. When the shock reaches the ν_e neutrinosphere near a radius of 100 km, the dammed-up ν_e's flood to infinity, the outer core is rapidly neutronized, and a trough in Y_e ($\sim$0.15) is formed (62, 63, 132). However, only the periphery of the core interior to the shock is neutronized; most of the inner core is at high densities and is still opaque and electron-rich. The neutronization of the entire core proceeds on the much longer time scales of hundreds of milliseconds to seconds characteristic of protoneutron star cooling.

The total ν_e energy radiated during the distinctive $\sim$5-ms breakout burst is only $\sim 2 \times 10^{51}$ ergs. The precise total energy depends on the details of the progenitor structure, with more massive cores yielding more breakout

ν_e's. The average ν_e energy ($\langle \varepsilon_{\nu_e} \rangle$) at breakout is $\sim$15 MeV and the ν_e spectrum changes abruptly from a capture to a pseudothermal one. This spectral transition, the few-millisecond duration of the spike, and its ν_e dominance are distinctive predictions of the modern theory. The harvest in detectors such as SNO or ICARUS of $\sim$100 breakout ν_e's from a collapse at 2 kpc might be enough to distinguish progenitor and explosion models.

Though ν_e's dominate the breakout spike, smaller ν_μ and $\bar{\nu}_e$ spikes also accompany shock emergence. When the shock reaches the ν_μ and $\bar{\nu}_e$ neutrinospheres (close to the ν_e neutrinosphere), the copious pairs generated in the shock-heated mantle escape. As Figure 2 demonstrates, the ν_μ and $\bar{\nu}_e$ light curves turn on quite abruptly, reaching luminosities of 10^{53} ergs s^{-1} and 2×10^{52} ergs s^{-1}, respectively, within a few tenths of milliseconds. The $\bar{\nu}_e$'s are partially suppressed by the positive electron-neutrino chemical potential that is a consequence of the e^-/e^+ asymmetry in the mantle (150, 151). However, μ_{ν_e} in the periphery decays with the formation of the Y_e trough. Because of this and the diffusion of heat via neutrinos from the outer shocked mantle ($10^{13} > \rho > 10^{11}$ g cm^{-3}), $L_{\bar{\nu}_e}$, as well as L_{ν_μ}, rises over a period of $\sim$20 ms to meet a falling L_{ν_e}. The characteristic time for this transient adjustment is the neutrino heat conduction time in the "thin" outer mantle, just interior to the neutrinospheres. Only a little more than 10 ms after bounce, the core reaches hydrostatic equilibrium and the ν_e excess moderates. Secondary peaks in $L_{\bar{\nu}_e}$ and L_{ν_μ} of 5×10^{52} ergs s^{-1} and 10^{53} ergs s^{-1}, respectively, are reached $\sim$25 ms after the breakout spike. Thereafter, L_{ν_e}, $L_{\bar{\nu}_e}$, and L_{ν_μ} decay roughly together.

The sharp turn-on and "gradual" rise to peak of the $\bar{\nu}_e$ and ν_μ emissions are important predictions of the general theory, though specifics change from model to model. An interesting feature observed in Figure 2 is the $\sim$20-ms period oscillation in all the luminosities from $\sim$130 to 160 ms and in L_{ν_e} and $L_{\bar{\nu}_e}$ through 220 ms, $\sim$110 ms after bounce. These oscillations result from the hydrodynamic pulsations of the outer mantle interior to a shock that has stalled at $\sim$200 km. L_{ν_μ} is less affected by mantle pulsation because the lower ν_μ cross sections push the ν_μ neutrinosphere deeper into the core, where the oscillation amplitudes (in radius and T) are smaller.

In the calculation of Myra & Burrows (120) represented in Figure 2, the energy of the bounce shock is sapped by dissociation and neutrino losses, and it stalls into accretion after $\sim$9 milliseconds. This is the standard problem with the prompt mechanism of supernovae that is presumably solved by re-energization on longer time scales (0.1–1.0 seconds) by core neutrinos (74, 78–80). The pulsations in L_ν seem to be signatures of a

stalled shock; they are absent when either a promptly successful or a late-time shock has swept the outer mantle of material that would otherwise be accreted through the shock onto the neutron star. Hence, oscillation in L_{ν_e} or $L_{\bar{\nu}_e}$ could be a useful diagnostic of the supernova mechanism (74, 79). The specific periods and amplitudes depend on the structure and mass of the progenitor core (e.g. 82), as does the duration of the pulsation phase.

The accretion of infalling matter through the stalled shock onto the protoneutron star can power a significant fraction of the early neutrino emissions, since the gravitational energy available per accreted baryon is roughly 100 MeV. The magnitude of this contribution depends on the core structure before collapse. However, according to the long-term scenario, once the shock has been revitalized, accretion is quickly reversed into explosion and ceases to fuel neutrino radiation. Figure 3 shows the radial motion of various mass zones in a calculation by Bethe & Wilson (80) that undergoes the long-term explosion (at $t = 0.5$ seconds) and illustrates the dramatic drop in accretion. The neutrino light curves should then show a charcteristic downward kink. In addition, the concomitant drastic thinning

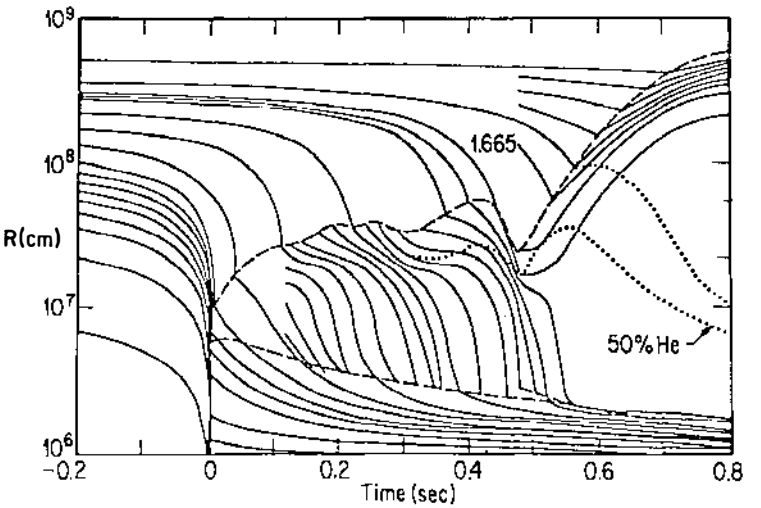

Figure 3 Plot of the radius (in centimeters) of selected mass zones versus time (in seconds) for the hydrodynamic calculation of Wilson (79). Time equals zero at bounce. Notice that the prompt shock stalls, but that after ~0.5 second the mantle lifts off the star and the supernova recommences. This is a "long-term" explosion. The 1.665 denotes the $1.665 M_\odot$ zone, "50% He" (*dotted*) signifies the separation line between alpha-rich (exterior) and alpha-poor (interior) zones. The lower *dashed line* marks the ν_e neutrinosphere and the upper *dashed line* denotes the shock wave. "Mantle collapse" after bounce is clearly seen.

of the outer mantle decreases the opacity and shifts the neutrinospheres inward to slightly higher temperatures. Therefore, the neutrino spectra harden, perhaps by ~20%, but the true magnitude of this effect is unclear (74, 75), and may be significantly less. Nevertheless, these discontinuities in the neutrino luminosities and average energies at shock revitalization are predictions of the long-term neutrino-mediated mechanism of supernova. Observing the magnitude and epoch of these model diagnostics would usefully constrain the theory.

The $\langle \varepsilon_{\nu_e} \rangle$ at breakout quickly settles from ~15 to ~10 MeV, a value it maintains with only a very slight (<5%) secular rise during the first 100 ms after bounce (Figure 2). Similarly, $\langle \varepsilon_{\bar{\nu}_e} \rangle$ settles at ~12.5 MeV and $\langle \varepsilon_{\nu_\mu} \rangle$ at ~24 MeV, and they too experience modest (<10%) secular rises. Nevertheless, these values are representative of the energy averages during much of the subsequent evolution. The value of $\langle \varepsilon_{\bar{\nu}_e} \rangle$ is higher than that of $\langle \varepsilon_{\nu_e} \rangle$ because the neutron-richness of the outer core makes the $\bar{\nu}_e(p, n)e^+$ opacity smaller than the $\nu_e(n, p)e^-$ opacity and allows us to see deeper into the core to higher temperatures in the $\bar{\nu}_e$ channel. Since the ν_μ's participate only in neutral-current interactions, similar arguments explain the still higher value of $\langle \varepsilon_{\nu_\mu} \rangle$. Figure 4 shows as solid lines the ν_μ, $\bar{\nu}_e$, and ν_e spectra

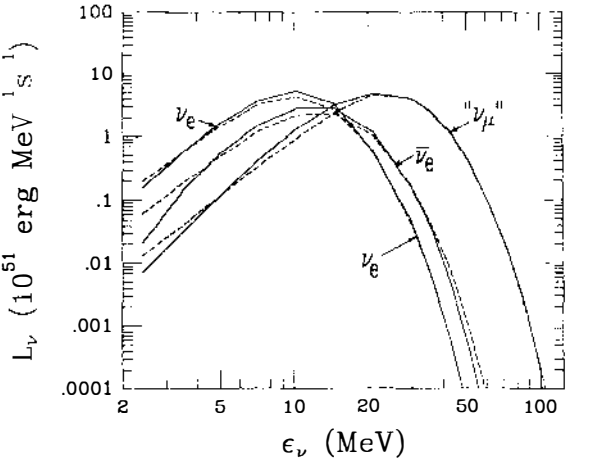

Figure 4 The ν_e, ν_μ, and $\bar{\nu}_e$ energy spectra at 43 ms after bounce, from the calculation of Myra & Burrows (120). The *solid lines* denote the calculated spectra in ergs MeV^{-1} s^{-1} versus ε_ν (in MeV), and the *dashed lines* are the best average-energy-preserving fits to a Fermi-Dirac distribution with a temperature (T_ν) and degeneracy parameter (η_ν). For ν_e, $\bar{\nu}_e$, and ν_μ the best-fit (T_ν, η_ν) are (2.4, 3.2), (3.1, 3.0), and (5.1, 4.1), respectively. Note that the spectra are naturally "pinched" with respect to an $\eta_\nu = 0$ spectrum: there is a deficit at both high and low energies. See text for discussion.

at 43 ms after bounce. Fermi-Dirac fits using a T_ν and η_ν ($=\mu_\nu/T_\nu$) that have no real physical meaning are superposed as dashed lines. The fitted values of (T_ν, η_ν) are (5.1 MeV, 4.1), (3.1 MeV, 3.0), and (2.4 MeV, 3.2) for ν_μ's, $\bar{\nu}_e$'s, and ν_e's, respectively.

The spectra in Figure 4 do not follow a zero-η_ν thermal distribution very well; they are "pinched" at both high and low energies (127, 128). Since the neutrino cross sections (Equations 2a–2d) are monotonically increasing functions of neutrino energy, the low energy part of a neutrino spectrum is depleted by transparency while the high energy part is truncated by opacity. The effective neutrinosphere of high energy ν's is thrust outward to low temperature regions.

The time-integrated spectra during the first 0.3 second after the bounce of a $1.27M_\odot$ core are given in Figure 5. Although $\langle\varepsilon_{\nu_\mu}\rangle$ in Figure 5 is a bit lower than that in Figure 4 and two different progenitors were employed, the spectra in Figures 4 and 5 are quite similar. They are

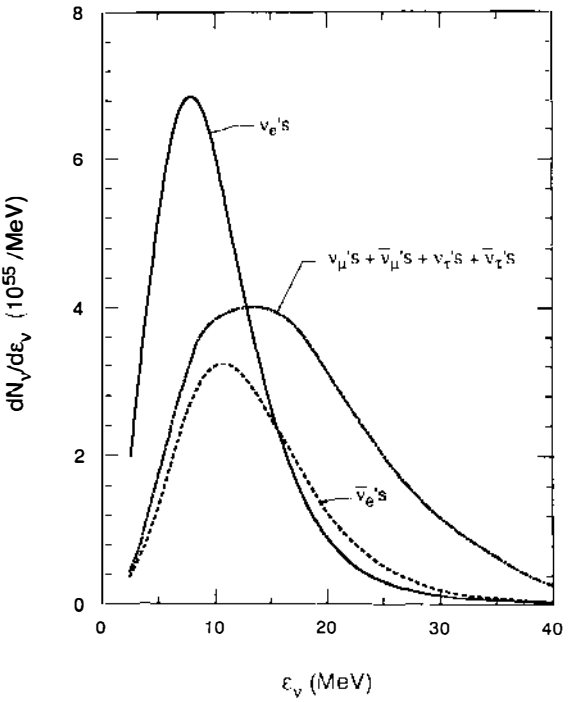

Figure 5 The time-integrated number spectra (in 10^{55} MeV^{-1}) of ν_e's. $\bar{\nu}_e$'s, and ν_μ's versus ε_ν (in MeV) from Bruenn (153). The integration was done through a post-bounce time of 0.3 second and the initial progenitor was a $1.27M_\odot$ core provided by Woosley et al (152).

also similar to those obtained by Woosley et al (76) at 1.0 second (after gravitational redshift corrections are applied). The depletion, both above and below the peak relative to a black body, is well fitted by a Fermi-Dirac distribution with a positive η_ν and a T_ν that is lower than would be obtained from the same average energy with $\eta_\nu = 0$. The deficit of high energy ν's has consequences for the long-term mechanism (154–156), neutrino nucleosynthesis in the outer shells of massive stars (157), and the detection of ν_μ's in the SNO heavy-water detector (13, 146).

5.2 *The Cooling and Neutronization of the Protoneutron Star*

Though much of the interesting and distinctive action during core evolution occurs during the early period followed in Figure 2, only $\sim 2 \times 10^{52}$ ergs were then radiated. This is only $\sim 10\%$ of the energy that must be radiated to form a cold neutron star. Fully 90% is still trapped in the hot, bloated, electron-rich core. This is the protoneutron star and it is during its quasi-hydrostatic shrinking, cooling, and neutronization that most of the neutrino signal of a supernova is generated. In fact, this phase emerges smoothly from the dynamical phase and lasts, not milliseconds, but seconds because of the profound neutrino opacity of the dense core. Heat and lepton number can be released only slowly by neutrino diffusion.

The initial radii of the protoneutron star ν_e and $\bar{\nu}_e$ neutrinospheres are near 80–100 km, while that of the ν_μ neutrinosphere is near 50 km (3, 63). The inner ~ 0.5–$0.7 M_\odot$ is at low entropy ($s \approx 1$) while the shocked outer 0.5–$0.7 M_\odot$ is at high entropy ($s \approx 7$–9), but the temperature starts near 5–10 MeV ($\sim 10^{11}$ K). The initial central density depends on the imperfectly known nuclear EOS (67, 129) and the initial core mass, but it is between 4.0 and 10.0×10^{14} g cm^{-3}. The densities near the neutrinospheres are near $10^{11\text{–}12}$ g cm^{-3} for the ν_e's and $\bar{\nu}_e$'s and near $10^{12.5}$ g cm^{-3} for the ν_μ's. The transparent material interior to the shock when it is at ~ 200 km is near 10^9 g cm^{-3}. Therefore, there is a steep negative density gradient from the center outward and a large contrast of thermodynamic regimes.

As described above, a trough in Y_e forms early (~ 10 ms) near the ν_e neutrinosphere. Both leptons and energy are rapidly radiated from the periphery because of the relatively low densities and opacities there. The quick loss of entropy and pressure support and the continued accretion lead to the quasi-hydrostatic collapse of the outer mantle on time scales of, perhaps, 100–200 ms. Curiously, the shock wave leaves the outer mantle convectively unstable (158–160). The effect of the instability on the rate of neutrino emission is as yet unknown but could be large (161).

The collapse of the mantle that attends this first stage of a protoneutron

star's neutrino energy loss is accompanied paradoxically by an increase in the matter temperature in these outer zones. This is a consequence of the negative specific heat effect of stars and the added weight of the accreted matter. As the mantle sinks, the gravitational energy change in the initially puffed out mantle is partitioned between neutrino emission and internal thermal energy. The temperatures of 30–50 MeV that can be achieved are the highest equilibrium temperatures seen in the universe after the big bang (or the last core collapse).

Figure 6 depicts the evolution of the temperature profile of an accreting protoneutron star during the first 30 seconds of its life (98). The "snapshots" are taken every 100 ms for the first two seconds and then every two seconds until $t = 30$ seconds. The compression spike can be seen first to grow rapidly (<1 s), then to diffuse into the center slowly (~ 10–15 s), and finally to decay.

The early mantle emission is a transient, because the initially rapid losses in the low density periphery cannot be sustained by the lower energy and lepton fluxes from the more opaque and dense interior. The luminosities

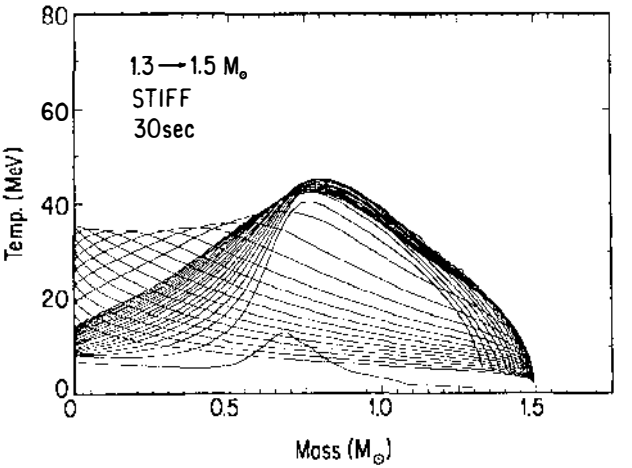

Figure 6 A collage of "snapshots" of the temperature (in MeV) versus enclosed baryon mass (in $M_\odot$) at various times in the life of a protoneutron star that starts at M(Baryon) $= 1.3M_\odot$ and fattens to $1.5M_\odot$ as a result of further accretion. These theoretical calculations were performed by Burrows (98) and employed a stiff nuclear EOS described by Burrows & Lattimer (3). The first snapshot ($t = 0$) is at the bottom. The subsequent snapshots are taken every 100 ms for 2.0 seconds and then every 2.0 seconds until $t = 30$ seconds. The temperature spike due to mantle collapse is clearly evident. Heat diffuses inward from this spike to warm the center to ~ 35 MeV. After ~ 16 seconds, the temperature, which is now monotonically decreasing with mass (and radius), decays gradually with a 10-second time constant.

adjust until the losses to infinity can be resupplied from the long-diffusion-time center. Therefore, protoneutron star emissions occur in two phases: (*a*) a mantle collapse phase that is modified by various rates of accretion and by the effects of convection and that can last tenths of seconds, and (*b*) a long diffusive phase that lasts for many seconds. The latter time scale is set by the product of the characteristic neutrino diffusion time and the ratio of the total thermal energy to the total neutrino energy. As most of the thermal energy is in nucleons and electrons, this ratio can be very large ($\sim$10–100). An estimate of this time scale can be obtained from

$$\tau_T = \frac{3R^2}{\pi^2 c\lambda}\left(\frac{E^0_{Th}}{2E^0_\nu}\right) \approx 10 \text{ seconds}, \qquad 3.$$

where R is $\sim$10 km; λ, a characteristic mean free path, is $\sim$10 meters; c is the speed of light; E^0_{Th} is the initial thermal energy; and E^0_ν is the initial neutrino energy. Equation 3 is very, very crude and ignores the density and opacity gradients, the difference between neutrino types, etc. However, it does give a rough estimate that is supported by more detailed stellar evolution calculations. The actual duration of this dominant phase depends upon the core mass, the EOS, and the problematic neutrino opacities in degenerate, strongly coupled neutron matter (96, 97).

The $\bar{\nu}_e$ luminosity evolution in the first 10 seconds for various protoneutron star models with varying degrees of accretion is given in Figure 7. The $\bar{\nu}_e$ luminosity starts near $\sim 10^{52}$ ergs s^{-1} as in Figure 2 and takes many seconds to decay to 10^{51} ergs s^{-1} (unless a black hole is formed, as in model 72 in Figure 7). Similar behavior is found for L_{ν_μ} and L_{ν_e}. The precise ratio of the luminosities in the different neutrino channels varies from calculation to calculation and from epoch to epoch. For instance, in Figure 2, L_{ν_μ}/L_{ν_e} at 0.1 second after bounce is $\sim$2, while in the calculations depicted in Figure 7, it is $\sim$4. It may be that this ratio is low at early times and evolves to rough equipartition between all the neutrino and antineutrino species within $\sim$1 second. Nevertheless, this rough equipartition is also seen in (75, 76). A good rule of thumb is that the total energy radiated is 5 ± 1 times the total $\bar{\nu}_e$ energy radiated.

A central drama of protoneutron star evolution is the conversion of degenerate ν_e's at 100–200 MeV in the dense, inner core into a mix of neutrinos of all six species at 10–30 MeV in the more tenuous outer envelope. As the degenerate ν_e's diffuse outward, they are down-scattered in energy. The matter through which they pass is heated and other neutrino species begin to carry some of the heat flux. In this way, lepton number and energy are transported simultaneously out of the star. The time scale for final neutronization is comparable to that for cooling. Figure 8 depicts

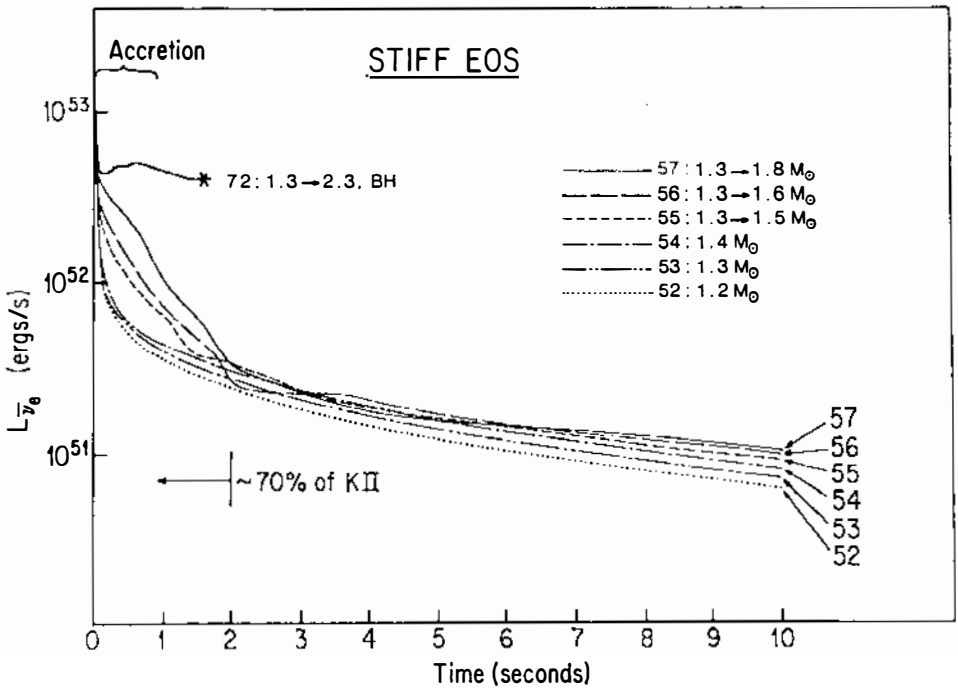

Figure 7 The $\bar{\nu}_e$ luminosity (in ergs s^{-1}) versus time (in seconds) for various protoneutron star models (with and without subsequent accretion) taken from (98), to which the reader is referred for details. The EOS employed is described in (3). The accretion phase is clearly marked, as is the epoch during which ~70% of the Kamiokande II signal occurred. Note that in model 72, accretion was so rapid that a black hole (BH) formed after less than two seconds. This suggests that a brief but high luminosity burst might signal the birth of a black hole. Such was certainly not so in SN1987A.

the evolution after bounce of the Y_ℓ profile with time. Note that the initial profile (in the background) has a trough in the periphery and that even after 10 seconds there are still many leptons left in the core. In this calculation, the neutron star is not a *neutron* star until roughly 20 seconds after bounce (foreground, $Y_\ell \approx Y_e \approx 0.04$; $Y_{\nu_e} \approx 0$).

6. THE NEUTRINOS FROM SN1987A

Few astronomical events in this century can or will rival Supernova 1987A as spectacle or science. However, its long list of impressive firsts reflects its relative proximity in the Large Magellanic Cloud (LMC), not an intrinsic

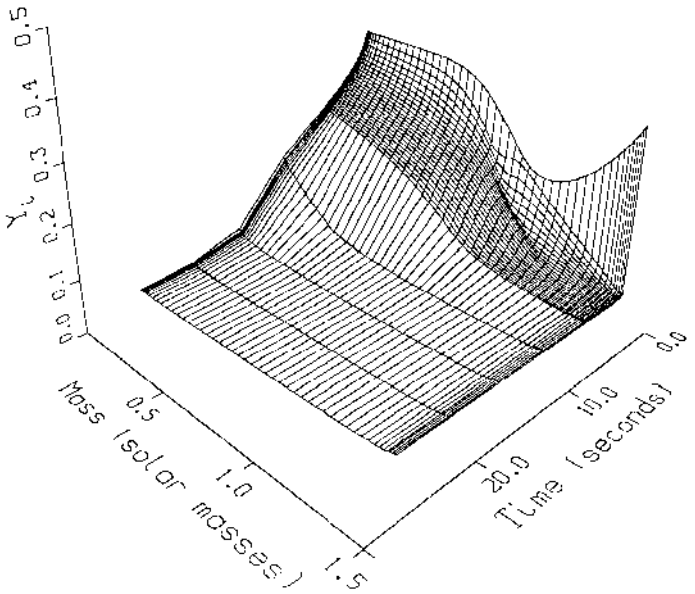

Figure 8 The lepton fraction ($Y_\ell = Y_e + Y_{\nu_e}$) per baryon versus enclosed baryon mass (in $M_\odot$) versus time (in seconds) for a $1.4M_\odot$ protoneutron star model, from (3). The total time depicted is 25 seconds. The line in the background is the Y_ℓ profile just after bounce ($t \approx 0$) and shows the trough expected at the stellar periphery. The figure clearly demonstrates the lethargy with which a young neutron star disgorges its leptons. It is only after ~ 20 seconds that neutron star Y_ℓ ($\approx Y_e$) values of ~ 0.04 are reached.

uniqueness. Nevertheless, it will long be remembered for its crowning first: the detection of the neutrinos (16, 17, 19, 22) long predicted. Within ~ 10 seconds on February 23.316 (UT), 1987, stellar collapse theory became an observational science and extragalactic neutrino astronomy was born. The importance of this has not been overlooked: over 300 papers on all aspects of the neutrino events now fill our libraries. Rather than survey, review, or recapitulate this literature, I summarize its major conclusions (see 13, 162–178). The brevity of this section reflects the sparseness of these neutrino data and the humility with which we should approach their interpretation. Crystal clarity must await the next galactic neutrino burst, with its superfluidity of events.

The epochal SN1987A neutrino data from the Irvine-Michigan-Brookhaven collaboration (IMB) (16, 179), Kamiokande II (KII) (17, 148), Baksan (19), and the Mont Blanc liquid scintillation detector (LSD) (22, 180) are depicted in Table 1. Shown are the event times, energies, and angles with respect to the LMC (where obtained). IMB and KII are water

Table 1 SN1987A neutrino data

Detector	Event number	Time[a] (seconds)	Electron energy (MeV)	Electron angle with respect to LMC (degrees)	Comment
IMB	1	7:35:41.374(UT)	38 ± 7	80 ± 10	± 50 ms
	2	0.411	37 ± 7	44 ± 15	
	3	0.650	28 ± 6	56 ± 20	
	4	1.141	39 ± 7	65 ± 20	
	5	1.562	36 ± 9	33 ± 15	
	6	2.683	36 ± 6	52 ± 10	
	7	5.010	19 ± 5	42 ± 20	
	8	5.581	22 ± 5	104 ± 20	
KII	1	7:35:35(UT)	20.0 ± 2.9	18 ± 18	± 1 min
	2	0.107	13.5 ± 3.2	40 ± 27	
	3	0.302	7.5 ± 2.0	108 ± 32	
	4	0.323	9.2 ± 2.7	70 ± 30	
	5	0.507	12.8 ± 2.9	135 ± 23	
	6	0.685	6.3 ± 1.7	68 ± 77	background
	7	1.540	35.4 ± 8.0	32 ± 16	
	8	1.728	21.0 ± 4.2	30 ± 18	
	9	1.915	19.8 ± 3.2	38 ± 22	
	10	9.219	8.6 ± 2.7	122 ± 30	
	11	10.432	13.0 ± 2.6	49 ± 26	
	12	12.439	8.9 ± 1.9	91 ± 39	
Baksan	1	7:36:11.818(UT)	12 ± 2.4		
	2	0.435	18 ± 3.6		
	3	1.710	23.3 ± 4.7		
	4	7.687	17 ± 3		
	5	9.099	20.1 ± 4.0		
Mont Blanc	1	2:52:36.792(UT)	7		IMB-4.7 hrs
	2	3.857	8		
	3	4.215	11		
	4	5.904	7		
	5	7.008	9		

[a] The UT times on February 23, 1987, are given for the first event; the time for each subsequent event is relative to the first.

Čerenkov detectors with fiducial masses for supernova detection of 5000 and 2140 tonnes and thresholds of 19 and 7.5 MeV, respectively. Baksan and LSD are scintillation detectors with fiducial masses of 200 and 90 tonnes and thresholds of 10 and 7 MeV, respectively. All four detectors are most sensitive to $\bar{\nu}_e$'s through the superallowed charged-current reaction on hydrogen (protons), $\bar{\nu}_e(p, n)e^+$. At 10 MeV, the neutrino-electron scattering cross section is at least a factor of 100 times lower than the $\bar{\nu}_e(p, n)e^+$ cross section.

The Mont Blanc data are problematical: not only did LSD detect its signal $\sim$4.7 hours earlier than IMB and KII, when these instruments detected nothing, but it detected as many as half their number of events, despite its diminutive size and sensitivity ($\sim 1/17 \times$ KII). A consistent model effectively excludes the possibility that what LSD saw were neutrinos from SN1987A. However, the scintillation technology developed for LSD is being profitably employed in the construction of the 3.6-kilotonne large-volume detector (LVD) (181, 182) in the Gran Sasso tunnel. If all goes well, the LVD should have a low threshold ($\sim$5 MeV) and exquisite sensitivity to a galactic collapse. The small size of the Baksan device makes its relatively large event yield curious, but not fatally so (21). The possibility that it detected SN1987A neutrinos cannot be excluded. For specificity, we focus below on the IMB and KII data and their implications.

The prediction (132–134) that 1–2 $\times 10^4$ $\bar{\nu}_e$ events can be expected in a water Čerenkov detector from a 1-kpc core collapse supernova per kilotonne of H_2O has been amply verified by the KII and IMB data, suitably scaled. The higher threshold and lower efficiency of the IMB detector completely accounts for its lower per-kilotonne yield (cf 98, 177). The large event angles in Table 1 imply that the majority were not ν-e^- scattering events, which are quite forward-peaked, but were indeed $\bar{\nu}_e$ events. However, the possibility that some small minority of these events were scatterings cannot be ignored (15, 183, 184). Though it is ironic that anti-electron-neutrino detection dominates in the context of neutronization and electron loss, such has been predicted for some time (e.g. 185). A good rule of thumb for any proposed underground neutrino burst detector is that we can expect some multiple of 10^4 events per kilotonne at 1 kpc, whatever the detector's composition or technology. What we have derived from IMB and KII about the internal physics of SN1987A and its neutrino burst is summarized as follows:

1. The event energies, number, and angles imply that most or all of them were $\bar{\nu}_e$ events.
2. The fluence of $\bar{\nu}_e$'s at the Earth was $5.0 \pm 2.5 \times 10^9$ cm^{-2}.
3. A zero chemical potential Fermi-Dirac fit to the event spectra yields a $T_{\bar{\nu}_e}$ of 4.0 ± 1.0 MeV and an average energy $\langle \varepsilon_{\bar{\nu}_e} \rangle$ of 12.5 ± 3.0 MeV. There is a slight indication of cooling with time.
4. The characteristic signal decay time (τ) is $\sim$4.0 seconds. There is some hint that the signal had two time constants, an early τ of $\sim$1 second and a later τ of $\sim$4.0 seconds.
5. During the early phase ($<$1 second), $L_{\bar{\nu}_e} \approx 4 \times 10^{52}$ ergs s^{-1}.
6. The core radius inferred from $T_{\bar{\nu}_e}$ and $L_{\bar{\nu}_e}$ and the blackbody assumption

is 30 ± 20 km. This is close to that of a classical neutron star and almost nothing else.

7. The total $\bar{\nu}_e$ energy radiated is $\sim 4 \pm 1 \times 10^{52}$ ergs, if $D = 50$ kpc is assumed.
8. The total energy radiated in all species is inferred from point 7 and theory to be $2 \pm 1 \times 10^{53}$ ergs. This is our first measurement of the binding energy of a neutron star.
9. The baryon and gravitational mass of the young neutron star can be inferred to be $1.45 \pm 0.15 M_\odot$ and $1.35 \pm 0.15 M_\odot$, respectively (cf 98).

The time scale, average energy, and total event number are gratifyingly close to the predictions of the modern theory described in the previous sections and are quite unlike the pre-1975 estimates. However, small number statistics will bedevil all who try to extract from Table 1 more than the fundamentals.

Particle physicists and others have delighted in using these neutrino data to derive constraints on the mass, charge, magnetic moment, and mean life of the $\bar{\nu}_e$ and the parameters of hypothetical particles such as axions (186) and majorons (187) that might have been generated in the proto-neutron star inferno. Good summaries of these attempts can be found in (12, 170, 177). Though nothing startling about neutrino properties was uncovered, the cleverness with which these few events were scrutinized and the multiplicity of uses to which they were put ensure that solid physics information cannot be avoided when hundreds of events from a galactic explosion are available.

The data displayed in Table 1 imply that ~ 1 nanogram mass equivalent of neutrinos passed through IMB and KII and that only 1 in 10^{15} of these were captured. This translates into ~ 500 grams of neutrinos through the entire Earth, roughly equivalent to 15 megatonnes of TNT. As many as one million people "experienced" an SN1987A $\bar{\nu}_e$ event in their bodies and ~ 300 experienced two. These curiosities serve to emphasize both the weak coupling of neutrinos to matter and the incredible magnitude of a collapse neutrino burst.

7. A GALACTIC NEUTRINO BURST

Both IMB and KII had completed essential detector upgrades no more than one year prior to the appearance of SN1987A. For these and for the fact that both were on line on February 23rd we should be grateful. However, neutrino bursts are sufficiently interesting and rare (10^{-2}–10^{-1} yr^{-1} in the Milky Way) that an international array of massive underground detectors with large data buffers and accurate timing seems indicated. Fortunately, the experimental community is now taking steps to establish such a network. In the near future SNO, Kamiokande, IMB, LVD,

Baksan, and, perhaps, ICARUS and DUMAND (188) will be providing continuous coverage of the neutrino sky. A collapse at the center of our galaxy ($\sim$8.5 kpc) will yield $\sim$1000 events in SNO, $\sim$500 events in both KII and IMB, a comparable number in LVD, and $\sim$150 events in ICARUS. Because of the large neutral-current cross sections on deuterium (189), the heavy-water detector, SNO, will be particularly sensitive to the "ν_μ" that are predicted to dominate the burst signal. Furthermore, both SNO and ICARUS promise to be singularly sensitive to the breakout burst of ν_e's.

The enthusiastic response to the meager neutrino yield from SN1987A has given us a glimpse of the reception with which a galactic supernova neutrino burst, with its plethora of events over scores of seconds, will be met. Detailed spectral, temporal, and flavor evolution of a supernova neutrino signal cannot but crack the supernova puzzle. The role of convection (161), rotation (190–192), and accretion will finally be clarified and a hundred things will be done routinely that the sensible did not dream even to attempt with the SN1987A data. To those of us who work in supernova theory, the anticipation is palpable.

ACKNOWLEDGMENTS

The author would like to thank Dave Arnett, John Bahcall, Hans Bethe, Gerry Brown, Steve Bruenn, Wolfgang Hillebrandt, Jim Lattimer, Ted Mazurek, Eric Myra, Ken Nomoto, Ray Sawyer, Dave Schramm, Jim Wilson, Stan Woosley, and Amos Yahil, among many others, for stimulating and useful conversations over the years. Special thanks are extended to the IMB and Kamioka collaborations for existing, and to Steve Bruenn and Eric Myra for providing work prior to publication. These efforts were supported in part by NSF Grants no. AST87-14176 and AST89-14346.

Literature Cited

1. Landau, L., *Phys. Z. Sowjetunion* 1: 285 (1932)
2. Baade, W., Zwicky, F., *Proc. Natl. Acad. Sci. USA* 20: 259 (1934)
3. Burrows, A., Lattimer, J. M., *Astrophys. J.* 207: 178 (1986)
4. Burbidge, E., Burbidge, G., Fowler, W. A., Hoyle, F., *Rev. Mod. Phys.* 29: 547 (1957)
5. Tammann, G., In *Supernovae: A Survey of Current Research*, ed. M. J. Rees, R. J. Stoneham. Dordrecht: Reidel (1982), p. 371
6. van den Bergh, S., McClure, R. D., Evans, R., *Astrophys. J.* 323: 44 (1989)
7. Ratnatunga, K. U., van den Bergh, S., *Astrophys. J.* 343: 713 (1989)
8. Evans, R., van den Bergh, S., McClure, D., *Astrophys. J.* 345: 752 (1989)
9. Cappellaro, E., Turatto, M., *Astron. Astrophys.* 190: 10 (1988)
10. Burrows, A., *Phys. Today* 40: 28 (1987)
11. Woosley, S. E., Phillips, M., *Science* 240: 750 (1988)
12. Arnett, W. D., Bahcall, J. N., Kirshner, R. P., Woosley, S. E., *Annu. Rev. Astron. Astrophys.* 27: 629 (1989)
13. Burrows, A., In *Supernovae*, ed. A. G. Petschek. Berlin: Springer-Verlag (1990), p. 143

14. Woosley, S. E., Weaver, T. A., *Annu. Rev. Astron. Astrophys.* 24: 205 (1986)
15. Bionta, R. M., Blewitt, G., Bratton, C. B., Cortez, B. G., Errede, S., et al., *Phys. Rev. Lett.* 51: 27 (1983)
16. Bionta, R. M., Blewitt, G., Bratton, C. B., Casper, D., *Phys. Rev. Lett.* 58: 1494 (1987)
17. Hirata, K., Kajita, T., Koshiba, M., Nakahata, M., Oyama, Y., et al., *Phys. Rev. Lett.* 58: 1490 (1987)
18. Hirata, K. S., Kajita, T., Koshiba, M., Nakahata, M., Oyama, Y., et al., *Phys. Rev.* D38: 448 (1988)
19. Alekseev, E. N., Alekseeva, L. N., Volchenko, V. I., Krivosheina, I. V., *Pis'ma Zh. Eksp. Teor. Fiz.* 45: 461 (1987)
20. Alekseev, E. N., Alekseeva, L. N., Volchenko, V. I., Krivosheina, I. V., *JETP Lett.* 45: 589 (1987)
21. Alekseev, E. N., Alekseeva, L. N., Krivosheina, I. V., Volchenko, V. I., *Phys. Lett.* B205: 209 (1988)
22. Aglietta, M., Badino, G., Bologna, G., Castagnoli, C., Castellina, A., et al., *Europhys. Lett.* 319: 136 (1987)
23. Aglietta, M., Badino, G., Bologna, G., Castagnoli, C., Casterllina, A., et al., *Europhys. Lett.* 319: 1321 (1987)
24. Chandrasekhar, S., *An Introduction to the Study of Stellar Structure.* Univ. Chicago Press (1939)
25. Hoyle, F., Fowler, W. A., *Astrophys. J.* 132: 565 (1960)
26. Fowler, W. A., Hoyle, F., *Astrophys. J. Suppl.* 9: 201 (1964)
27. Bodenheimer, P., Woosley, S. E., *Astrophys. J.* 269: 281 (1983)
28. Chiu, H. Y., *Phys. Rev.* 123: 1040 (1961)
29. Chiu, H. Y., *Ann. Phys.* 26: 364 (1964)
30. Colgate, S. A., White, R. H., *Astrophys. J.* 143: 626 (1966)
31. Arnett, W. D., *Can. J. Phys.* 44: 2553 (1966)
32. Arnett, W. D., *Can. J. Phys.* 45: 1621 (1967)
33. Colgate, S. A., Johnson, H. J., *Phys. Rev. Lett.* 5: 235 (1960)
34. Baym, G., Bethe, H. A., Pethick, C. J., *Nucl. Phys.* A175: 225 (1971)
35. Lattimer, J. M., Mackie, F., Ravenhall, D. G., Schramm, D. N., *Astrophys. J.* 213: 255 (1977)
36. Lattimer, J. M., Pethick, C. J., Ravenhall, G., Lamb, D. Q., *Nucl. Phys.* A432: 646 (1985)
37. Mazurek, T. J., Lattimer, J. M., Brown, G. E., *Astrophys. J.* 238: 139 (1979)
38. Bethe, H. A., Brown, C. F., Applegate, J., Lattimer, J. M., *Nucl. Phys.* A324: 487 (1979)
39. Bethe, H. A., *Annu. Rev. Nucl. Part. Sci.* 38: 1 (1988)
40. Van Riper, K. A., *Astrophys. J.* 326: 235 (1988)
41. Bruenn, S. W., *Astrophys. J.* 341: 385 (1989)
42. Feynman, R. P., Gell-Mann, M., *Phys. Rev.* 109: 193 (1958)
43. Bahcall, J. N., *Phys. Rev.* B136: 1164 (1964)
44. Bahcall, J. N., Frautschi, S. C., *Phys. Rev.* B136: 1547 (1964)
45. Beaudet, G., Petrosian, V., Salpeter, E., *Astrophys. J.* 150: 979 (1967)
46. Dicus, D., *Phys. Rev.* D6: 941 (1972)
47. Freedman, D. Z., *Phys. Rev.* D9: 1389 (1974)
48. Tubbs, D., Schramm, D., *Astrophys. J.* 201: 467 (1975)
49. Freedman, D. Z., Schramm, D. N., Tubbs, D. L., *Annu. Rev. Nucl. Sci.* 27: 167 (1977)
50. Weaver, T. A., Zimmerman, G. B., Woosley, S. E., *Astrophys. J.* 225: 1021 (1978)
51. Woosley, S. E., Weaver, T. A., *Astrophys. J.* 238: 1017 (1980)
52. Nomoto, K., *Astrophys. J.* 277: 791 (1984)
53. Weaver, T. A., Woosley, S. E., Fuller, G. M., In *Numerical Astrophysics, Proc. Symp. in honor of James R. Wilson, Univ. Illinois, Oct. 1982*, ed. J. M. Centrella, J. M. LeBlanc, R. L. Bowers. Boston: Jones & Bartlett (1985), p. 374
54. Woosley, S. E., Weaver, T. A., In *Radiation Hydrodynamics in Stars and Compact Objects*, ed. D. Mihalas, K. H. A. Winkler. Berlin: Springer-Verlag (1986), p. 91
55. Iben, I., Renzini, A., *Annu. Rev. Astron. Astrophys.* 21: 271 (1983)
56. Schinder, P. J., Schramm, D. N., Wiita, P. J., Margolis, S. H., Tubbs, D. L., *Astrophys. J.* 313: 531 (1987)
57. Itoh, N., Adachi, T., Nakagawa, M., Kohyama, Y., Munakata, H., *Astrophys. J.* 339: 354 (1989)
58. Goldreich, P., Weber, S. V., *Astrophys. J.* 238: 991 (1980)
59. Yahil, A., *Astrophys. J.* 265: 1047 (1983)
60. Van Riper, K. A., Lattimer, J. M., *Astrophys. J.* 249: 270 (1981)
61. Lattimer, J. M., *Annu. Rev. Nucl. Part. Sci.* 31: 337 (1981)
62. Van Riper, K. A., *Astrophys. J.* 221: 304 (1978)
63. Bowers, R. B., Wilson, J. R., *Astrophys. J.* 263: 366 (1982)
64. Burrows, A., Lattimer, J., *Astrophys. J. Lett.* 299: L15 (1989)

65. Lattimer, J. M., Burrows, A., Yahil, A., *Astrophys. J.* 288: 644 (1985)
66. Myra, E., Bludman, S. A., Hoffman, Y., Lichtenstadt, I., Sack, N., Van Riper, K. A., *Astrophys. J.* 318: 744 (1986)
67. Baron, E., Cooperstein, J., Kahana, S., *Phys. Rev. Lett.* 55: L126 (1985)
68. Hillebrandt, W., *Astron. Astrophys.* 110: L3 (1982)
69. Takahara, M., Sato, K., *Prog. Theor. Phys.* 68(3): 795 (1983)
70. Burrows, A., Lattimer, J., *Astrophys. J.* 270: 735 (1983)
71. Hillebrandt, W., Müller, E., *Astron. Astrophys.* 103: 147 (1981)
72. Mazurek, T. J., *Astrophys. J. Lett.* 259: L13 (1982)
73. Burrows, A., Mazurek, T. J., Lattimer, J. M., *Astrophys. J.* 251: 325 (1981)
74. Mayle, R., PhD thesis. Univ. Calif., Berkeley (*UCRL preprint no. 53713*) (1985)
75. Mayle, R., Wilson, J. R., Schramm, D. N., *Astrophys. J.* 318: 288 (1987)
76. Woosley, S. F., Wilson, J. R., Mayle, R., *Astrophys. J.* 302: 19 (1986)
77. Wilson, J., *Astrophys. J.* 163: 209 (1971)
78. Lattimer, J. M., Burrows, A., In *Problems of Collapse and Numerical Relativity*, ed. D. Bancel, M. Signore. Dordrecht: Reidel (1984), p. 147
79. Wilson, J. R., See Ref. 53, p. 422
80. Bethe, H. A., Wilson, J. R., *Astrophys. J.* 295: 14 (1985)
81. Bruenn, S. W., *Astrophys. Space Sci.* 143: 15 (1988)
82. Bruenn, S. W., *Astrophys. J.* 340: 955 (1989)
83. Bruenn, S. W., *Astrophys. J. Suppl.* 58: 771 (1985)
84. Bruenn, S. W., *Astrophys. J. Suppl.* 62: 331 (1986)
85. Lamb, D. Q., Lattimer, J. M., Pethick, C. J., Ravenhall, D. G., *Nucl. Phys.* A360: 459 (1981)
86. Fuller, G., *Astrophys. J.* 252: 741 (1982)
87. Fuller, G., Fowler, W. A., Newman, M., *Astrophys. J. Suppl.* 42: 447 (1980)
88. Cooperstein, J., Wambach, J., *Nucl. Phys.* A420: 591 (1984)
89. Zaringhalam, A., *Nucl. Phys.* A404: 599 (1983)
90. Aufderheide, M., Brown, G. E., Kuo, T. T. S., Stout, B., Vogal, P., *Nucl. Phys.* In prcss (1990)
91. Mazurek, T. J., *Nature* 252: 287 (1974)
92. Sato, K., *Prog. Theor. Phys.* 57: 1325 (1975)
93. Arnett, W. D., *Astrophys. J.* 218: 815 (1977)
94. Sehgal, I., *Nucl. Phys.* B70: 61 (1974)
95. Goodwin, B. T., *Astrophys. J.* 261: 321 (1982)
96. Goodwin, B. T., Pethick, C. J., *Astrophys. J.* 253: 816 (1982)
97. Iwamoto, N., Pethick, C. J., *Phys. Rev.* D25: 313 (1982)
98. Burrows, A., *Astrophys. J.* 334: 891 (1988)
99. Lamb, D. Q., Pethick, C. J., *Astrophys. J. Lett.* 209: L77 (1976)
100. Tubbs, D., *Astrophys. J. Suppl.* 37: 287 (1978)
101. Burrows, A., Mazurek, T. J., *Astrophys. J.* 259: 330 (1982)
102. Wilson, J., *Phys. Rev. Lett.* 32: 849 (1974)
103. Wilson, J. R., *Proc. Int. Sch. Phys., Enrico Fermi*, 65: 644 (1978)
104. Cooperstein, J., *Phys. Rep.* 163: 95 (1988)
105. Mazurek, T. J., *Ap. Space Sci.* 35: 117 (1975)
106. Mazurek, T. J., *Astrophys. J. Lett.* 207: L87 (1976)
107. Mazurek, T. J., *Comments Ap. Space Sci.* 7: 77 (1977)
108. Epstein, R. I., Pethick, C. J., *Astrophys. J.* 243: 1003 (1981)
109. Lattimer, J. M., Ravenhall, D. G., *Astrophys. J.* 223: 314 (1978)
110. Schwartz, R. A., *Am. Phys.* 37: 487 (1967)
111. van den Horn, L. J., Cooperstein, J., *Astrophys. J.* 300: 142 (1986)
112. Baron, E., Myra, E., Cooperstein, J., van den Horn, L., *Astrophys. J.* 339: 978 (1989)
113. Cooperstein, J., van den Horn, L. J., Baron, E., *Astrophys. J.* 309: 653 (1986)
114. Bludman, S., Van Riper, K. A., *Astrophys. J.* 224: 631 (1978)
115. Imshennik, V. S., Nadyozhin, D. K., *Sov. Phys. JETP* 36: 821 (1973)
116. Imshennik, V. S., Nadyozhin, D. K., *Astrophys. Space Sci.* 62: 309 (1979)
117. Nadyozhin, D. K., Otroshenko, I. V., *Astron. Zh.* 57: 78 (1980)
118. Salpeter, E. E., Shapiro, S. L., *Astrophys. J.* 251: 311 (1981)
119. Bruenn, S. W. 1975. *Ann. NY Acad. Sci.* 262: 80 (1975)
120. Myra, E., Burrows, A., *Astrophys. J.* In press (1990)
121. Lichtenstadt, I., Ron, A., Sack, N., Wagschal, J. J., Bludman, S. A., *Astrophys. J.* 226: 22 (1978)
122. Yueh, W. P., Buchler, J. R., *Ap. Space Sci.* 39: 429 (1976)
123. Schinder, P. J., Shapiro, S. L., *Astrophys. J.* 259: 311 (1982)
124. Schinder, P. J., Shapiro, S. L., *Astrophys. J. Suppl.* 50: 23 (1982)

125. Schinder, P. J., *Phys. Rev.* D38: 1673 (1988)
126. Mellor, P., Chière, J. P., Basdevant, J. L., *Astron. Astrophys.* 197: 123 (1988)
127. Giovanoni, P. M., Ellison, D. C., Bruenn, S. W., *Astrophys. J.* 342: 416 (1989)
128. Janka, H.-T., Hillebrandt, W., *Astron. Astrophys. Suppl.* 78: 375 (1989)
129. Glenndenning, N., *Phys. Rev.* C37: 2733 (1988)
130. Sawyer, R. F., Scalapino, D. J., Soni, A., In *Neutrino-79*, ed. V. Berger. Singapore: World Sci. (1979), p. 429
131. Sawyer, R., *Astrophys. J.* 234: 1085 (1980)
132. Burrows, A., Mazurek, T. J., *Nature* 301: 315 (1983)
133. Burrows, A., In *Solar Neutrinos and Neutrino Astronomy*, ed. M. L. Cherry, W. A. Fowler, K. Lande (AIP Conf. Proc. 126) (1984), p. 283
134. Burrows, A., *Astrophys. J.* 283: 848 (1984)
135. LoSecco, J. M., *Science* 224: 56 (1983)
136. Hillebrandt, W., In *Proc. Conf. High Energy Phenomena Around Collapsed Stars, Cargese, France, Sept. 1985, NATO ASI Series C*, ed. F. Pacini. Dordrecht: Reidel (1987), p. 73
137. Nadyozhin, D. K., *Astrophys. Space Sci.* 51: 283 (1978)
138. Nadyozhin, D. K., *Astrophys. Space Sci.* 53: 131 (1978)
139. Nadyozhin, D. K., *Astrophys. Space Sci.* 2: 75 (1983)
140. Imshennik, V. S., Nadyozhin, D. K., *Astrophys. Space Sci. Rev.* 2: 75 (1983)
141. Domogatsky, G. V., Zatsepin, G. T., In *Proc. 9th Int. Conf. on Cosmic Rays* 2: 1030 (1965)
142. Zatsepin, G. I., *JETP Lett.* 8: 205 (1968)
143. Bruenn, S. W., *Phys. Rev. Lett.* 59: 938 (1987)
144. Blinnikov, S. I., Imshennik, V. S., Nadyozhin, D. K., In *Neutrino-88*, ed. J. Schneps, T. Kafka, W. A. Mann, Pran Nath. Singapore: World Sci. (1988), p. 165
145. Nomoto, K., Hashimoto, M., *Phys. Rep.* 163: 13 (1988)
146. Sinclair, D., et al., *Nuovo Cimento* C9: 308 (1986)
147. Cline, D., In *Proc. Workshop on Extra Solar Neutrino Astronomy, Observational Neutrino Astronomy*, ed. D. Cline. Singapore: World Sci. (1988), p. 233
148. Koshiba, M., In *ICOBAN '84, Park City, Utah, Jan. 1984*
149. Koshiba, M., In *Proc. 23rd Rencontre de Moriond, Les Arcs, Savoie, France, Jan. 21–28, 1988*, ed. O. Fackler, J. Tran Thanh Van. Singapore: Ed. Front. (1988), p. 215
150. Bethe, H. A., Applegate, J. H., Brown, G. E., *Astrophys. J.* 241: 343 (1980)
151. Bethe, H. A., Yahil, A., Brown, G., *Astrophys. J. Lett.* 262: L7 (1982)
152. Woosley, S. E., Pinto, P., Ensman, L., *Astrophys. J.* 324: 466 (1988)
153. Bruenn, S. W. 1990. Preprint
154. Ray, A., Kar, K., *Phys. Rev. Lett.* 63: 2435 (1989)
155. Haxton, W., *Phys. Rev.* D36: 2283 (1987)
156. Haxton, W., *Phys. Rev. Lett.* 60: 1999 (1988)
157. Woosley, S. E., Hartmann, D. H., Hoffman, R. D., Haxton, W. C., *Astrophys. J.* In press (1990)
158. Epstein, R. I., *Mon. Not. R. Astron. Soc.* 188: 305 (1979)
159. Lattimer, J. M., Mazurek, T. J., *Astrophys. J.* 246: 995 (1981)
160. Smarr, L., Barton, S., Bowers, R. L., Wilson, J. R., *Astrophys. J.* 246: 515 (1981)
161. Burrows, A., *Astrophys. J. Lett.* 318: L57 (1987)
162. Arafune, J., Fukugita, M., *Phys. Rev. Lett.* 59: 367 (1987)
163. Arnett, W. D., *Astrophys. J.* 319: 136 (1987)
164. Bahcall, J. N., Dar, A., Piran, T., *Nature* 326: 135 (1987)
165. Bahcall, J. N., Piran, T., Press, W. H., Spergel, D. N., *Nature* 327: 682 (1987)
166. Bludman, S. A., Schinder, P. J., *Astrophys. J.* 326: 265 (1988)
167. Burrows, A., Lattimer, J., *Astrophys. J. Lett.* 318: L63 (1987)
168. Joutras, D., Cline, D., *Astrophys. Lett. Comments* 26: 341 (1988)
169. Kahana, S., Cooperstein, J., Baron, E., *Phys. Lett.* B196: 259 (1987)
170. Krauss, L. M., *Nature* 329: 689 (1987)
171. Lamb, D. Q., Melia, F., Loredo, T. J., In *Supernova 1987A in the Large Magellanic Cloud*, ed. M. Kafatos, A. Michalitsianos. Cambridge Univ. Press (1988), p. 204
172. Lattimer, J. M., *Nucl. Phys.* A478: 199 (1988)
173. Lattimer, J. M., Yahil, A., *Astrophys. J.* 340: 426 (1989)
174. Sato, K., Suzuki, H., *Phys. Rev. Lett.* 58: 2722 (1987)
175. Sato, K., Suzuki, H., *Phys. Lett.* B196: 267 (1987)
176. Schaefer, R., Declais, Y., Julian, S., *Nature* 330: 142 (1987)
177. Schramm, D. N., *Comments Nucl. Part. Phys.* 17: 239 (1987)
178. Spergel, D. N., Piran, T., Loeb, A.,

Goodman, J., Bahcall, J. N., *Science* 237: 1471 (1987)
179. Badino, G., et al., *Nuovo Cimento* 7C: 573 (1984)
180. Aglietta, M., Badino, G., Bologna, G. F., Castagnoli, C., Fulgione, W., et al., *Nuovo Cimento* 9C: 185 (1986)
181. Pless, I. See Ref. 149, p. 309
182. Pless, I. See Ref. 144, p. 297
183. LoSecco, J. M., *Phys. Rev.* D39: 1013 (1989)
184. Kielczewska, D., *Phys. Rev.* D. In press (1990)
185. Frati, W., et al., *Ann. NY Acad. Sci.* 262: 219 (1975)
186. Burrows, A., Turner, M. S., Brinkmann, R. P., *Phys. Rev.* D39: 1020 (1989)
187. Goldman, I., Aharonov, Y., Alexander, G., Nussinov, S., *Phys. Rev. Lett.* 60: 1789 (1988)
188. Pryor, C., Roos, C. E., Webster, M. S., *Astrophys. J.* 329: 335 (1988)
189. Ying, S., Haxton, W., Henley, F. M., In *Proc. WEIN-89*, ed. P. Depommier. Singapore: Ed. Front. (1990), p. 715
190. Janka, H.-T., Mönchmeyer, R., *Astron. Astrophys.* 209: L5 (1988)
191. Mönchmeyer, F., Müller, E., In *NATO ASI on Timing Neutron Stars*, ed. H. Ögelman, E. van den Heuvel. Dordrecht: Reidel (1989), p. 549
192. Wilson, J., LeBlanc, J. M., *Astrophys. J.* 161: 541 (1970)